Mutational Evidence for Control of Cell Adhesion Through Integrin Diffusion/Clustering, Independent of Ligand Binding

By Robert L. Yauch,* Dan P. Felsenfeld,§ Stine-Kathrein Kraeft,‡ Lan Bo Chen,‡ Michael P. Sheetz,§ and Martin E. Hemler*

*From the *Division of Tumor Virology, and the ‡Division of Molecular and Cellular Biology, Dana-Farber Cancer Institute, Boston, Massachusetts 02115; and the §Department of Cell Biology, Duke University Medical Center, Durham, North Carolina 27710*

Summary

Previous studies have shown that integrin α chain tails make strong positive contributions to integrin-mediated cell adhesion. We now show here that integrin α^4 tail deletion markedly impairs static cell adhesion by a mechanism that does not involve altered binding of soluble vascular cell adhesion molecule 1 ligand. Instead, truncation of the α^4 cytoplasmic domain caused a severe deficiency in integrin accumulation into cell surface clusters, as induced by ligand and/or antibodies. Furthermore, α^4 tail deletion also significantly decreased the membrane diffusivity of $\alpha^4\beta_1$, as determined by a single particle tracking technique. Notably, low doses of cytochalasin D partially restored the deficiency in cell adhesion seen upon α^4 tail deletion. Together, these results suggest that α^4 tail deletion exposes the β_1 cytoplasmic domain, leading to cytoskeletal associations that apparently restrict integrin lateral diffusion and accumulation into clusters, thus causing reduced static cell adhesion. Our demonstration of integrin adhesive activity regulated through receptor diffusion/clustering (rather than through altered ligand binding affinity) may be highly relevant towards the understanding of inside–out signaling mechanisms for β_1 integrins.

Cell adhesion is a critical event in the initiation and maintenance of a wide array of physiological processes, including embryogenesis, hematopoiesis, tumor cell metastasis, and the immune response. The integrin protein family, which consists of 22 distinct α and β heterodimers, mediates cell adhesion to extracellular matrix proteins, serum proteins, and counterreceptors on other cells (1). Through inside–out signaling, integrin adhesive activity can be triggered by multiple agonists, and integrins display multiple activation states within different cell types, independent of changes in integrin expression levels (2). Many studies of integrin regulation have focused on conformational changes, altered ligand binding affinity, and/or modulation of postligand binding events (e.g., cell spreading) (3–6). However, a novel mechanism was recently put forth, suggesting that activation of adhesion may involve release of cytoskeletal constraints, leading to increased integrin lateral mobility (7, 8). Implicit is the assumption that increased mobility is proadhesive because it leads to increased integrin accumulation at an adhesive site, and thus greater adhesion strengthening.

Here, we have used an α^4 integrin cytoplasmic domain mutant to provide strong evidence for this hypothesis. Upon truncation of the α^4 cytoplasmic domain, the $\alpha^4\beta_1$ integrin shows severe impairments in both constitutive and phorbol ester–induced static cell adhesion (9, 10), and also shows deficient adhesion strengthening under shear (11, 12). However, the reason for these defects was not previously understood. Because other integrin cytoplasmic domain mutations cause altered ligand binding (3, 13, 14), we closely examined binding of soluble vascular cell adhesion molecule (VCAM)-1[1] (15) to mutant and wild-type $\alpha^4\beta_1$ integrin. Not finding any alterations in ligand binding, we then examined receptor accumulation into cell surface clusters, and integrin lateral mobility. The results strongly support the hypothesis that integrin diffusion/clustering, independent of alterations in ligand binding, can play a major role in regulating integrin adhesive functions.

Materials and Methods

Cells. K562 erythroleukemia cells and Chinese hamster ovary (CHO) cells transfected with cDNAs representing the wild-type

[1]*Abbreviations used in this paper:* AP, alkaline phosphatase; CHO, Chinese hamster ovary; FBS, fetal bovine serum; MSD, mean square displacement; rsVCAM, recombinant soluble vascular cell adhesion molecule; TBS, Tris-buffered saline; VCAM, vascular cell adhesion molecule.

 J. Exp. Med. © The Rockefeller University Press • 0022-1007/97/10/1347/09 $2.00
Volume 186, Number 8, October 20, 1997 1347–1355
http://www.jem.org

human α^4 integrin ($-\alpha^4$wt), chimeric α^4 containing the extracellular and transmembrane domains of α^4 with the cytoplasmic domain of α^2 (-X4C2), and a truncated α^4 integrin lacking a cytoplasmic domain (-X4C0), have been described elsewhere (9). Untransfected or mock-transfected K562 and/or CHO cells were used as negative controls. K562 transfectants were maintained in RPMI-1640 containing 10% fetal bovine serum (FBS), 1 mg/ml G418 sulfate (GIBCO BRL, Gaithersburg, MD), and antibiotics, whereas CHO transfectants were maintained in MEMα^- media containing 10% dialyzed FBS, 0.5 mg/ml G418 sulfate, and antibiotics.

Reagents and Antibodies. The antibodies used in this study include anti-α^4, B5G10 (16), and A4-PUJ1 (17); anti-CD32 (anti-FcγRII), 4.6.19 (18); fluorescein-conjugated goat anti–mouse IgG (Cappel, Westchester, PA); fluorescein-conjugated goat anti–mouse κ (Caltag, San Francisco, CA); negative control mAb J-2A2 (19); and mAb 15/7, recognizing a β_1 epitope induced by manganese or ligand (20). Fluoresceinated B5G10 was produced using *N*-hydroxy succinimide (NHS)–fluorescein (Pierce, Rockford, IL), as described by the manufacturer. Recombinant soluble VCAM (rsVCAM) and alkaline phosphatase (AP)–conjugated VCAM–Ig (VCAM–Ig–AP) were a gift from Dr. Roy Lobb (Biogen, Inc., Cambridge, MA) and prepared as described elsewhere (15). The VCAM–Ig–AP contains the two NH_2-terminal domains of human VCAM fused to the hinge, CH2, and CH3 domains of human IgG1. A purified VCAM–mouse C κ chain fusion protein (VCAM-κ) was a gift from Dr. Philip Lake (Sandoz Co., East Hanover, NJ). VCAM-κ was produced as a soluble protein from sf9 cells and contains all seven human VCAM domains, except the transmembrane and cytoplasmic domains, which have been replaced by a 100–amino acid mouse C κ segment. The CS-1 peptide (GPEILDVPST) derived from fibronectin was synthesized at the Dana-Farber Molecular Biology Core facility (Boston, MA).

Flow Cytometry. Flow cytometric assays were performed as described (21). For determination of 15/7 epitope expression, K562 cells were preincubated (10 min) with 2 mM EDTA (in PBS), washed and suspended in assay buffer (24 mM Tris, 137 mM NaCl, 2.7 mM KCl, pH 7.4 [Tris-buffered saline; TBS], 5% BSA, 0.02% NaN_3) with or without $MnCl_2$ and/or CS-1 peptide. Then, mAb 15/7 or negative control mAb J-2A2 was added and mean fluorescence intensities were determined. Results for 15/7 expression are given as a percent of $\alpha^4\beta_1$ levels (% 15/7 = [15/7 − J2A2]/[A4-PUJ1 − J2A2] × 100). Untransfected K562 cells (expressing the $\alpha^5\beta_1$ integrin) showed no constitutive or divalent cation-induced 15/7 expression.

VCAM–Ig–AP Direct Ligand Binding Assay. A detailed description of a high sensitivity, direct ligand binding assay has been described elsewhere (15). In brief, cells in 96-well porous plates were incubated with a VCAM–Ig fusion protein conjugated with AP (VCAM–Ig–AP), and then washed using a Millipore Multiscreen filtration manifold. Bound VCAM–Ig–AP was then detected by colorimetric assay using *p*-nitrophenyl phosphate.

VCAM-κ Indirect Ligand Binding Assay. Transfected K562 cells were incubated for 10 min on ice with TBS containing 2 mM EDTA, washed three times with assay buffer (TBS, 2% BSA), and resuspended in assay buffer containing the desired concentrations of VCAM-κ and either $MnCl_2$ or 5 mM EDTA. Cells were incubated at 4°C for 30 min, washed two times in assay buffer containing 2 mM $MnCl_2$, and subsequently incubated for 30 min at 4°C with assay buffer containing fluorescein-conjugated goat anti–mouse κ antibodies. Cells were washed two times and fixed with 3% paraformaldehyde. VCAM-κ binding on K562 cells was analyzed using a FACScan® flow cytometer to give mean fluorescence intensity units. Background binding of VCAM-κ (i.e., VCAM-κ binding in the presence of 5 mM EDTA) was subtracted and data were also corrected for α^4 surface expression, if applicable.

Cell Adhesion. The effects of cytochalasin D on cell adhesion were performed as previously described (7), with minor modifications. In brief, BCECF-AM (Molecular Probes, Eugene, OR) –labeled cells were pretreated with various doses of cytochalasin D (Sigma Chemical Co., St. Louis, MO) for 15 min at 37°C. Cells were added to 96-well plates previously coated overnight with α^4 ligands and blocked with 0.1% heat-denatured BSA for 45 min at 37°C. Plates were centrifuged at 500 rpm for 2 min and analyzed in a Cytofluor 2300 measurement system (Millipore Corp., Bedford, MA). Plates were incubated for an additional 15 min at 37°C, washed 3–4 times with adhesion media, and fluorescence was reanalyzed. Background binding to heat-denatured BSA alone was typically <5% and was subtracted from experimental values. Data is expressed as fold induction in cell adhesion, and calculated (adhesion in the presence of cytochalasin D/adhesion in the absence of cytochalasin D) from triplicate cultures.

Confocal Microscopy. K562 cells were incubated on ice for 10 min in PBS containing 2 mM EDTA, washed, and resuspended in assay buffer (TBS, 5% BSA, 0.02% NaN_3). For examination of VCAM-induced clustering of α^4, cells were incubated with 5 μg/ml of mAb 4.6.19 to block FcγRII sites, and then with 500 nM rsVCAM and 2 mM $MnCl_2$ in assay buffer for 45 min. Cells were washed two times in assay buffer containing 2 mM $MnCl_2$, incubated an additional 30 min in assay buffer containing fluoresceinated B5G10 mAb, washed, and fixed with 4% paraformaldehyde in PBS. For detection of α^4 clustering induced by secondary antibodies, K562 cells were incubated for 30 min in assay buffer (PBS substituted for TBS) containing purified B5G10, washed, incubated an additional 30 min with fluorescein-conjugated goat anti–mouse IgG, washed, and fixed as above. All procedures were done at 4°C in the presence of 0.02% NaN_3 to prevent internalization. Fixed cells were resuspended in Fluorosave reagent (Calbiochem Novabiochem, La Jolla, CA), mounted onto slides, and fluorescence was analyzed using a Zeiss model LSM4 confocal laser scanning microscope equipped with an external argon–krypton laser (488 nm). To evaluate cell surface fluorescence, optical sections of 0.5-μm thickness were taken at the center and at the cell membrane of representative cells. Images of 512 × 512 pixels were digitally recorded within 4 s and printed with a Kodak 8650 PS color printer, using Adobe Photoshop software (Adobe Systems, Mountain View, CA).

Analysis of $\alpha^4\beta_1$ Diffusion. 40-nm colloidal gold particles (EY Laboratories, San Mateo, CA) were coated with antibody using a biotin–avidin linkage as described (22). In brief, gold particles were coated with ovalbumin (20 μg/ml gold suspension) at pH 4.7, followed by blocking with 0.05% PEG 20K. After washing (three times with 0.05% PEG 20K/PBS; 16.5K *g* for 10 min), particles were reacted with NHS–LC–biotin (20 μg/ml gold; Pierce) overnight on ice. Particles were subsequently washed three times (0.05% PEG 20K in PBS) and incubated with avidin neutralite (Molecular Probes; 1 mg/ml gold, starting volume) for 3 h on ice. The gold solution was then washed three times as described above and incubated for 3 h with biotin–B5G10 (60 μg/ml gold, starting volume) and blocked with 1 mg BSA biotinamido caproyl (Sigma) overnight on ice.

CHO cells were cultured on silane-blocked coverslips (23) coated with vitronectin (5 μg/ml). Video experiments were carried out in phenol red–free MEM α supplemented with 2 mM

l-glutamine, 10% FCS, and 20 mM Hepes. Gold particles were added to cell-conditioned culture medium and culture dishes were sealed before mounting on a Zeiss Axiovert 100 TV inverted microscope equipped with Nomarski optics and a NA 1.3 100× plan neofluar objective. Serial, recorded video frames were digitized and analyzed for particle centroid position using previously published nanometer-resolution techniques (24).

Mean square displacement (MSD) with respect to time was calculated for each particle centroid trace and two-dimensional diffusion coefficients were calculated by fitting MSD curves with the equation MSD = $4Dt + v^2t^2$ or by linear regression of the first 0.5 s of the MSD curve (25). *P* values were calculated using Student's *t* test.

Results

Previously, it was shown that deletion of the α^4 cytoplasmic domain markedly decreased $\alpha^4\beta_1$–dependent adhesion of several cell types to multiple ligands (9–12). Here, we sought to determine whether this mutation also altered the ability of $\alpha^4\beta_1$ to bind soluble ligand. Wild-type α^4 (-α^4 wt), truncated α^4 (-X4C0), and a chimeric α^4 containing the cytoplasmic domain of α^2 (-X4C2) were stably expressed at comparable levels on the surface of both K562 erythroleukemia and CHO cells (Fig. 1). In a direct ligand binding assay (Fig. 2 *A*), comparable binding of an AP-conjugated VCAM–Ig fusion protein was seen for cells expressing wild-type α^4, truncated α^4, or chimeric α^4. The concentration of VCAM–Ig–AP yielding half-maximal direct ligand binding activity (ED_{50}) was 1–1.5 nM for all three K562 transfectants, consistent with previously published results showing ED_{50} values of ~1 nM (15). Again, no essential difference between wild-type and mutant α^4 was obtained in an indirect binding assay, using fluorescein-conjugated goat anti–mouse κ antibodies to detect bound VCAM-κ (Fig. 2 *B*). Minimal nonspecific binding of either VCAM–Ig–AP or VCAM-κ was detected on mock-transfected K562 cells, confirming that binding is α^4 integrin-dependent (Fig. 2, *A* and *B*).

Ligand binding was carried out in 2 mM manganese, because calcium and magnesium (either alone, or together, at ~ 1–2 mM) fail to support binding of soluble VCAM (15, 26). To alleviate concern that manganese might mask differences in VCAM binding by inducing high affinity $\alpha^4\beta_1$ (15, 26, 27), manganese was titrated over a range of concentrations, whereas VCAM was held constant at 4 nM VCAM–Ig–AP (Fig. 2 *C*), or 500 nM VCAM-κ (Fig. 2 *D*). Manganese stimulated VCAM binding that was dose-

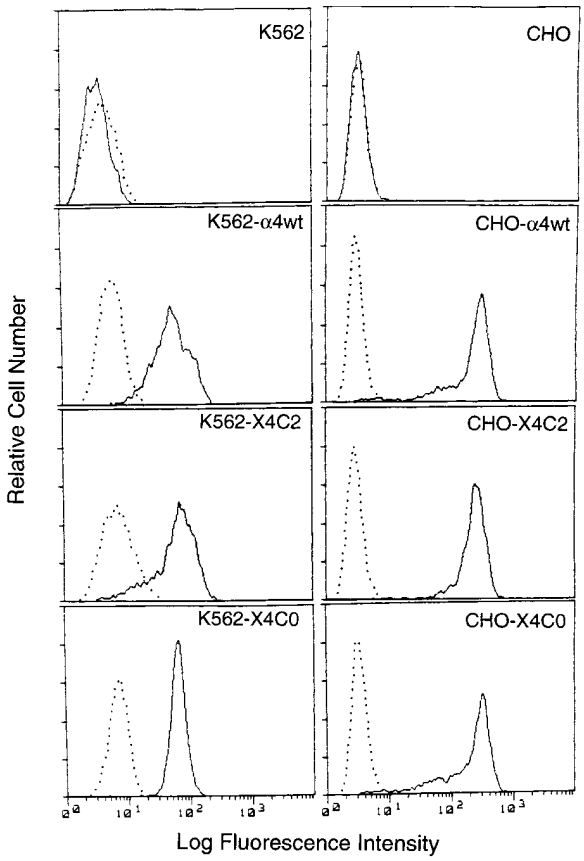

Figure 1. Expression of α^4 cytoplasmic tail mutants on K562 and CHO cells. Cells transfected with vector alone (*top row*) or with wild-type α^4, -X4C2, or -X4C0 were stained with a negative control mAb, P3 (*dotted line*), or with anti-α^4 mAb, A4-PUJ1 (*solid line*). Mean fluorescence intensity shown in logarithmic scale was determined by flow cytometry, as described in Materials and Methods. Heterodimer assembly was not altered by α^4 tail deletion or substitution (9).

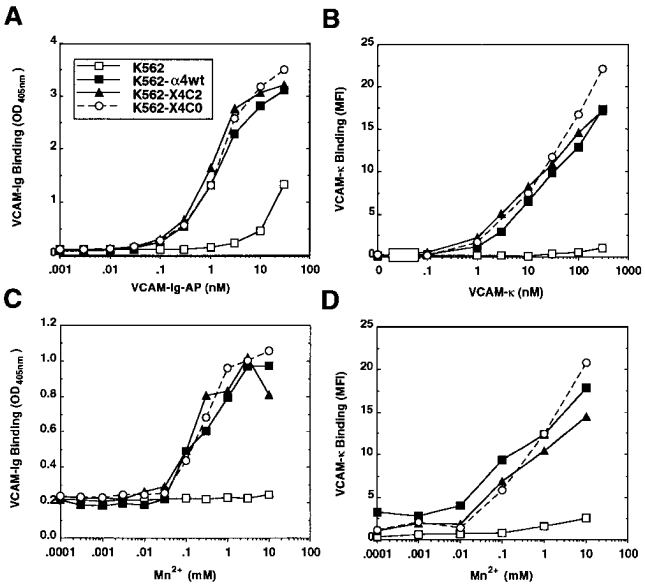

Figure 2. Analysis of VCAM binding to K562 α^4 transfectants by direct (*A* and *C*) and indirect (*B* and *D*) ligand binding assays. Recombinant VCAM fusion proteins were cultured with mock-transfected or various α^4-transfected K562 cells at 4°C, as described in Materials and Methods. Direct binding of VCAM–Ig–AP was determined while varying ligand (*A*) in the presence of 2 mM $MnCl_2$, or by varying Mn^{2+} (*C*) in the presence of 4 nM VCAM–Ig–AP. Bound VCAM was determined from AP activity, measured at OD_{405}. Indirect VCAM-κ binding was analyzed by varying ligand (*B*) in the presence of 2 mM $MnCl_2$ and by varying divalent cation (*D*) in the presence of 500 nM VCAM-κ. Fluorescein-conjugated goat anti–mouse κ IgG was used to determine the level of VCAM-κ bound and results are expressed as mean fluorescence intensities (*MFI*). The combined data are representative of six individual experiments.

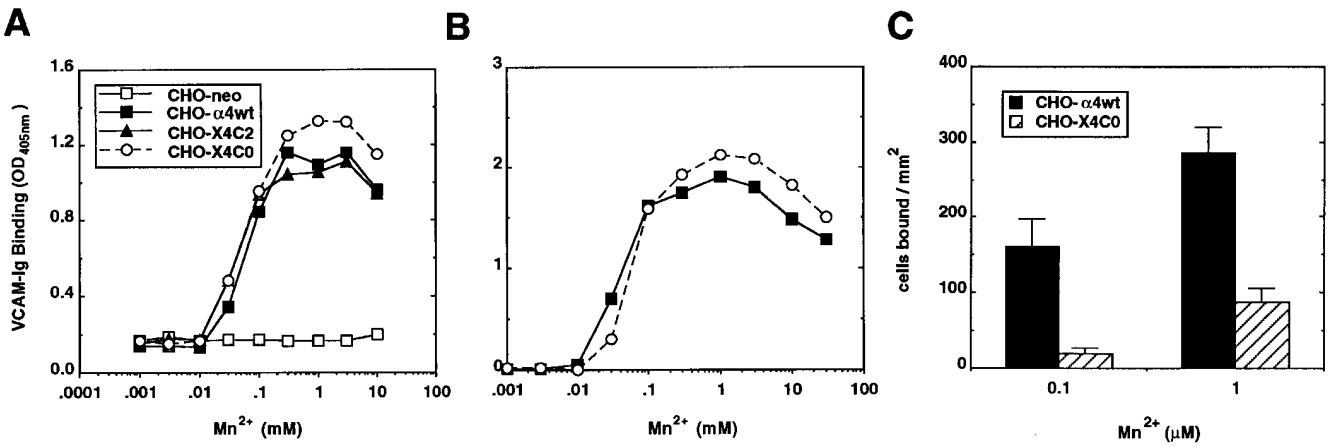

Figure 3. Effect of Mn^{2+} on binding of soluble VCAM (*A* and *B*) and adhesion to immobilized VCAM (*C*) in CHO α^4 transfectants. Direct binding of VCAM–Ig–AP to α^4-transfected CHO cells was determined while varying the divalent cation concentration in the presence of an optimal (*A*; 4 nM VCAM–Ig–AP) or suboptimal (*B*; 1 nM VCAM–Ig–AP) dose of ligand, as described in Fig. 2. $OD_{405\ nm}$ values were higher in *B* due to longer substrate development times. The data are representative of four experiments. The adhesion of CHO cell transfectants to rsVCAM, coated at 2 μg/ml (*C*), was carried out as described previously (9, 10).

dependent and α^4-specific, but again no differences were apparent between K562–α4wt, K562–X4C2 and, K562–X4C0 cells (Fig. 2, *C* and *D*).

In CHO cells, compared with K562 cells, $\alpha^4\beta_1$ is constitutively more active with respect to mediating cell adhesion (9, 10). Nonetheless, in the CHO cellular environment, there were again no differences in direct VCAM binding to α^4wt and X4C0 integrins at either optimal (Fig. 3 *A*; 4 nM VCAM–Ig–AP) or suboptimal (Fig. 3 *B*; 1 nM VCAM–Ig–AP) doses of ligand. Half-maximal direct VCAM–Ig–AP binding occurred at ~100 μM manganese for all transfectants examined, consistent with previously published manganese ED_{50} values for VCAM–$\alpha^4\beta_1$ binding (15). In contrast with ligand binding, cell adhesion to immobilized VCAM was markedly diminished for CHO–X4C0 cells, compared with α^4wt cells (Fig. 3 *C*). For example, adhesion at 0.1 and 1 μM Mn^{2+} was reduced by 88 and 69%, respectively.

To examine α^4 tail deletion effects on very late antigen 4 conformation, we used the mAb 15/7, which recognizes a β_1 integrin conformation induced by ligand occupancy or manganese. When 15/7 epitope is induced by manganese, it correlates with increased ligand binding affinity (20). However, the 15/7 epitope also appears when the β_1 cytoplasmic domain is deleted, and ligand binding is diminished (28). Notably, 15/7 epitope expression is most readily induced on $\alpha^4\beta_1$, as compared with other β_1 integrins (Bazzoni, G., L. Ma, M.L. Blue, and M.E. Hemler, manuscript submitted for publication), and thus is an especially useful tool for evaluating altered $\alpha^4\beta_1$ conformations.

Negligible 15/7 epitope expression was seen for α^4wt and mutant α^4 integrins in K562 cells in the absence of stimulation (Table 1). However, the percentage of $\alpha^4\beta_1$ molecules expressing the 15/7 epitope increased dramatically upon addition of CS-1 peptide or manganese or both together to the K562–α^4wt and K562–X4C2 cells. Importantly, stimulation with manganese and/or CS-1 peptide also resulted in comparably increased 15/7 epitope on K562–X4C0 cells (Table 1). No 15/7 epitope was detected in mock-transfected K562 cells (stimulated or unstimulated), demonstrating that 15/7 was specifically reporting $\alpha^4\beta_1$ conformational changes.

Having found that α^4 tail deletion does not alter ligand binding or integrin conformation, we then sought alternative explanations for why tail deletion impairs cell adhesion. To this end, confocal laser microscopy was used to examine α^4 tail deletion effects on accumulation of $\alpha^4\beta_1$ in clusters. As illustrated, wild-type α^4 (Fig. 4 *d*) and X4C2 (Fig. 4 *c*) were detected in clusters on the surface of K562 cells after addition of recombinant soluble VCAM in the presence of manganese. In sharp contrast, X4C0 showed hardly any VCAM-induced accumulation in clusters (Fig. 4 *b*). The X4C0 subunit was present on the cell surface at levels comparable to α^4wt and X4C2 (see Fig. 1), suggesting that differences in signal strength reflect aggregated receptor and not differences in total receptor number. Cell

Table 1. *15/7 Epitope Expression on K562 Transfectants*

	Percent of $\alpha^4\beta_1$ expressing 15/7*			
Cell line	No stimulation	CS-1	Mn^{2+}	CS-1 + Mn^{2+}
K562	0	0	0	0
K562–α^4wt	0	36	45	64
K562–X4C2	3.6	62	69	71
K562–X4C0	0	56	64	70

*15/7 expression was determined in the presence of no divalent cations or ligand (no stimulation), 100 μM CS-1 peptide, 5 mM $MnCl_2$, or 5 mM $MnCl_2$ + 100 μM CS-1. Results are presented as the percent of $\alpha^4\beta_1$ expressing the 15/7 epitope, as described in Materials and Methods.

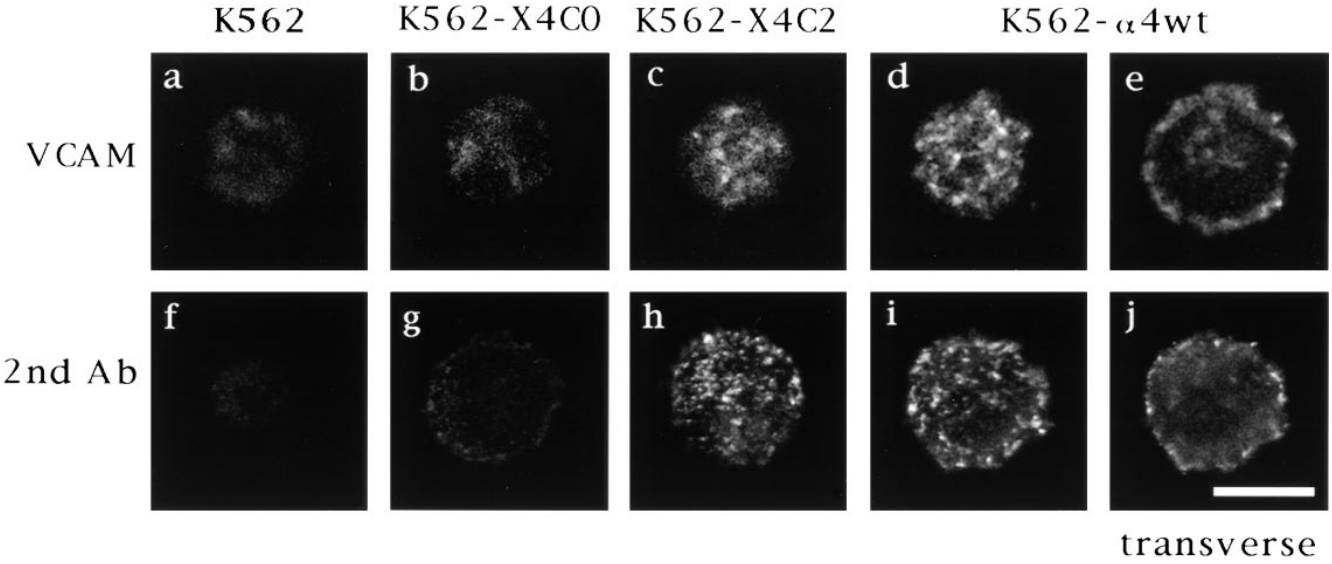

Figure 4. Clustering of α^4 on the surface of K562 cells as examined by confocal microscopy. (*a–e*) Mock-transfected and α^4-transfected K562 cells were pretreated with antibodies to FcγRII and subsequently incubated at 4°C with 500 nM rsVCAM in the presence of 2 mM $MnCl_2$. Then, ligand-induced α^4 distribution was determined by adding fluorescein-conjugated anti-α^4 mAb B5G10, followed by confocal microscopy. The data are representative of four individual experiments. (*f–j*) Untransfected and α^4-transfected K562 cells were incubated at 4°C with the anti-α^4 mAb B5G10, and then clustering was induced by adding a secondary fluorescein-conjugated goat anti–mouse IgG. The data are representative of six individual experiments. *e* and *j* represent transverse sections, whereas all other images represent surface sections. Bar, 10 μm.

surface staining was specific for α^4, as shown by the lack of staining on mock-transfected K562 cells (Fig. 4 *a*). The distribution of α^4 into clusters was dependent upon the addition of VCAM, because manganese alone (at 2 mM) did not induce clustering of α^4 (data not shown).

Experiments were carried out at 4°C in the presence of sodium azide to prevent receptor internalization. Transverse sections of K562–α^4wt cells (Fig. 4 *e*) showed peripheral, but not intracellular staining, consistent with cell surface clustering without receptor internalization. Also, transverse sections of K562–X4C0 cells showed no evidence for intracellular staining (data not shown). Furthermore, levels of cell surface α^4 (X4C0) were unaltered after incubation with VCAM, as determined by flow cytometry (data not shown).

To extend our findings, we also examined α^4 clustering induced by anti-α^4 mAb, followed by polyclonal secondary antibody (Fig. 4, *f–j*). As indicated, clustering was again pronounced on K562–α^4wt (Fig. 4, *i* and *j*) and K562–X4C2 (Fig. 4 *h*) cells, whereas minimal clustering was observed when the α^4 tail was deleted (K562–X4C0 cells; Fig. 4 *g*) or when no α^4 was present (Fig. 4 *f*). Results in Fig. 5, showing 9–15 cells/panel, confirm the single cell results shown in Fig. 4. As indicated, nearly all of the K562–α^4wt cells exhibit pronounced clustering, induced either by VCAM (Fig. 5 *a*) or by antibody (Fig. 5 *c*). In contrast, the X4C0 mutant was much less clustered (Fig. 5, *b* and *d*), despite being expressed on the cell surface at levels nearly equivalent to α^4wt (see Fig. 1).

The failure of truncated α^4 to form cell surface clusters raises the possibility that increased or altered associations with the underlying cytoskeleton may impair the lateral mobility of truncated α^4, restricting its redistribution into a cluster. Because restricted lateral movement of integrin receptors will likely be reflected by a lower integrin diffusion rate (22, 23), next we directly measured the diffusion coefficients of wild-type and truncated α^4 in CHO transfectants at 37°C. The two-dimensional diffusivity of 40-nm gold particles, coated with anti-α^4 mAb, was measured on the lamellipodia of CHO–α^4wt and CHO–X4C0 cells spread on an α^4-independent substrate, vitronectin. Movement of gold particles was viewed by high magnification, video-enhanced differential interference contrast microscopy and particles were tracked by computer with nanometer-level accuracy (23). A nonperturbing anti-α^4 mAb, B5G10, was used because this mAb neither blocks nor stimulates $\alpha^4\beta_1$-mediated functions (29). It was shown elsewhere that nonperturbing antibodies coupled to 40-nm gold can report the random diffusion of integrins without stimulating the cross-linking and directed movement of these receptors (22).

As illustrated in Fig. 6, *A* and *C*, gold particles bound to the lamella of CHO–α^4wt cells diffused freely with a mean diffusion coefficient of 0.03 $\mu m^2/s$ (Fig. 6 *E*), consistent with the diffusion rate observed for other β_1 integrins (22), as well as other cell surface glycoproteins (30). However, truncation of the α^4 cytoplasmic domain resulted in a significant decrease in the $\alpha^4\beta_1$ diffusion rate ($P < 0.01$). Particles bound to CHO–X4C0 cells exhibited reduced lateral mobility (Fig. 6, *B* and *D*), with a diffusion coefficient that was sixfold lower (0.005 $\mu m^2/s$) than wild-type $\alpha^4\beta_1$. No binding of gold particles was detected on mock-transfected CHO cells, demonstrating that the binding is $\alpha^4\beta_1$ specific (data not shown).

The association of integrins with cytoskeletal elements can restrain the random diffusivity of integrins and thus

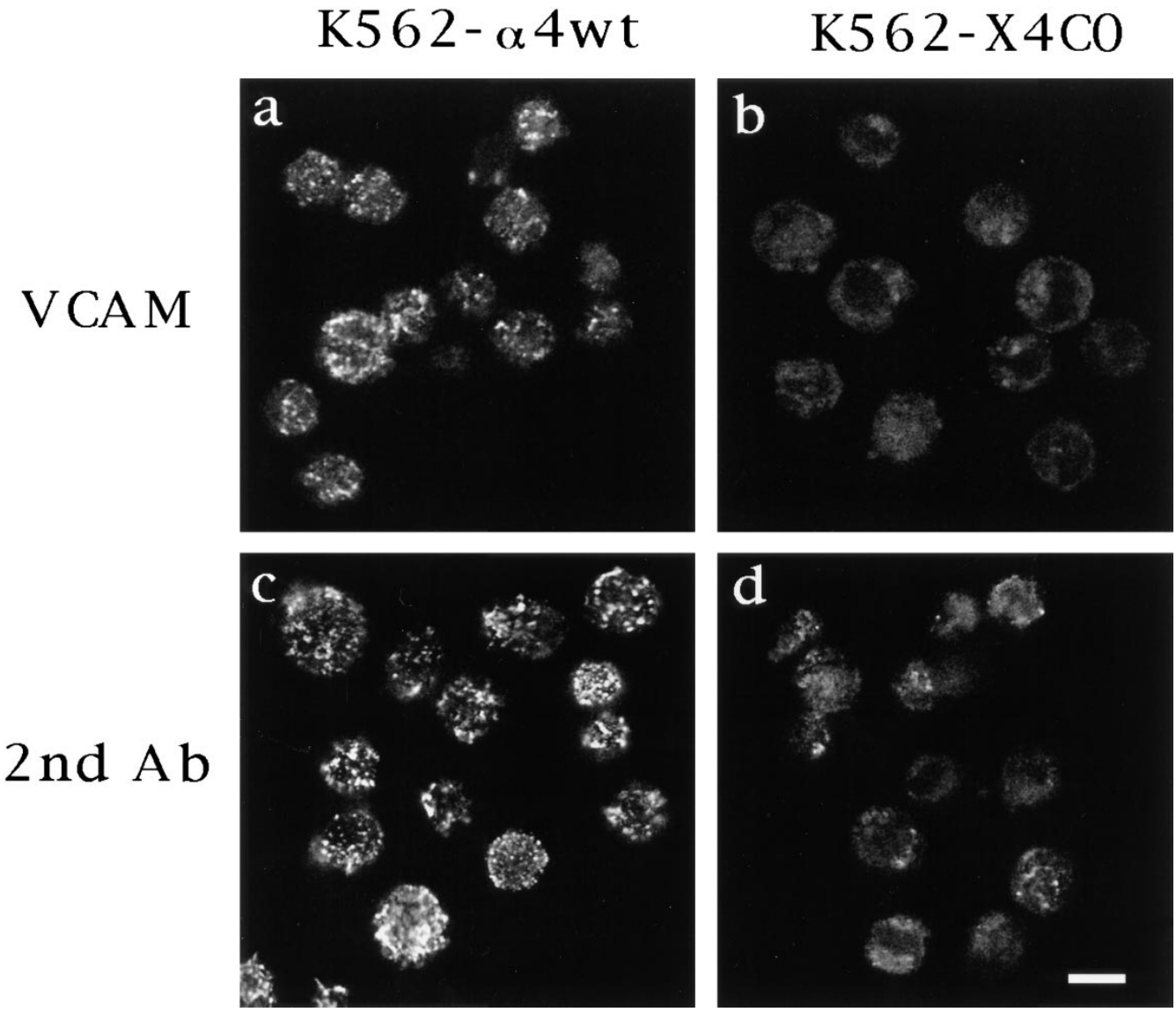

Figure 5. Distribution of α^4 on multiple K562–α^4wt and K562–X4C0 cells. Confocal microscopy was used to examine the cell surface distribution of α^4 upon treatment of K562–α^4wt (*a* and *c*) and K562–X4C0 (*b* and *d*) transfectants with soluble VCAM (*a* and *b*) or with secondary antibodies (*c* and *d*), as described in Fig. 4. Bar, 10 μm.

contribute to a diminished adhesive state (7). To examine whether the actin cytoskeleton may contribute to the deficiency in adhesion mediated by truncated α^4, we disrupted actin filament organization with cytochalasin D and measured its effect on $\alpha^4\beta_1$–mediated adhesion. At high doses (>10 μg/ml) of cytochalasin D, adhesion of both CHO–α^4wt and CHO–X4C0 to α^4 ligands was dramatically reduced (data not shown), as seen many times previously. However, at low doses, cytochalasin D stimulated markedly the adhesion of CHO–X4C0 cells to two different α^4 ligands, FN40 (Fig. 7 *A*) and VCAM (Fig. 7 *B*), without much increasing the adhesion of wild-type α^4 transfectants. Adhesion was α^4 specific, as mock-transfected CHO cells did not adhere under these conditions (data not shown).

Discussion

Although α^4 tail deletion has a profound negative effect on cell adhesion (9, 10; Fig. 3 *C*), and on adhesion strengthening under shear conditions (11, 12), we show here that it does not alter ligand binding. Ligand binding was unaltered by α^4 tail deletion (*a*) as measured either directly or indirectly, (*b*) as measured on either K562 cells or CHO cells, and (*c*) as shown either by manganese titration (at constant ligand) or by ligand titration (at constant manganese). Previous results also suggested that α^4 tail deletion did not alter ligand binding, but that study was done only indirectly, and under single cation conditions, on a single cell line (18). In addition, α^4 tail deletion was shown previously not to alter cell tethering in hydrodynamic flow (11,

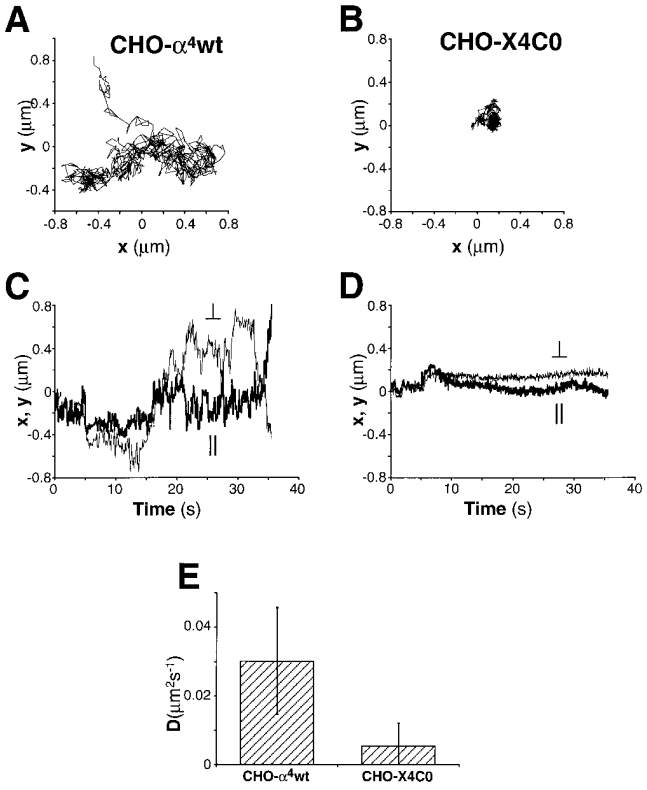

Figure 6. Analysis of α^4 integrin diffusivity in α^4-transfected CHO cells. 40-nm gold particles coated with nonperturbing, anti-α^4 mAb (B5G10) were bound to the surface of α^4-transfected CHO cells and tracked in the plane of the membrane at 37°C, as described in Materials and Methods. Representative tracks (*x* versus *y*; μm) are shown for particles on CHO–α^4wt (*A*) and CHO–X4C0 (*B*). All tracks were rotated to orient cell with leading edge facing left. Also, *x* and *y* coordinates with respect to time are shown for CHO–α^4wt (*C*) and CHO–X4C0 (*D*) cells (*x* coordinates, *fine line*, ⊥; *y* coordinates, *bold line*, ∥). (E) Two-dimensional diffusivity (*D*; $\mu m^2/s$) determined from a plot of MSD versus time of particles tracked on CHO–α^4wt ($n = 6$) and CHO–X4C0 ($n = 9$) transfectants ($P < 0.01$). Data are represented as mean deviation ± SD. No binding of anti-α^4-coated particles was detected on mock-transfected CHO cells.

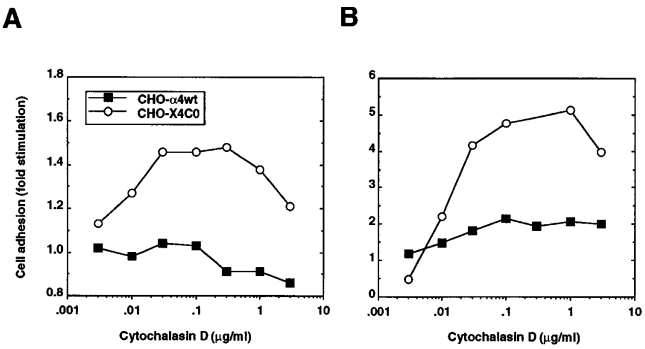

Figure 7. Effect of cytochalasin D on adhesion of α^4-transfected CHO cells to α^4 ligands. BCECF-AM–labeled CHO–α^4wt (*closed squares*) or CHO–X4C0 (*open circles*) were pretreated with various concentrations of cytochalasin D for 15 min at 37°C and subsequently allowed to adhere to surfaces coated at 4 μg/ml of FN40 (*A*) or 2 μg/ml of rsVCAM (*B*), as described in Materials and Methods. Results are presented as fold increases in adhesion calculated due to the presence of cytochalasin D. Actual adhesion values in the absence of cytochalasin D were 104.2 cells bound/mm² for CHO–α^4wt and 22.8 cells bound/mm² for CHO–X4C0 on VCAM, respectively.

12), a function that is likely dependent on univalent integrin–ligand bond formation. Thus, our results argue strongly against affinity modulation as a mechanism for α^4 tail regulation of cellular adhesion. Consistent with these findings, α^4 tail deletion also did not decrease the ability of divalent cations or ligand to induce $\alpha^4\beta_1$ conformations detected by mAb 15/7. Similarly, α^4 tail deletion was shown previously to have no effect on induction of an epitope defined by mAb 9EG7 (10), that maps to a β_1 site distinct from the 15/7 site (28, 31).

It is, perhaps, not surprising that replacement of the α^4 tail with the α^2 tail had no effect on ligand binding or integrin conformation, because previously that mutation had no effect on cell adhesion, or tethering under flow (9, 12). Notably, replacement of the α^{IIb} cytoplasmic domain with that of α^2 did cause an increase in $\alpha^{IIb}\beta_3$ integrin ligand binding (14), suggesting that different rules may apply to regulation of the $\alpha^{IIb}\beta_3$ integrin.

The defect in cell adhesion seen for the X4C0 mutant is not due to altered ligand binding, but rather appears to arise from a reduced diffusion rate. Presumably, a lower rate of diffusion prevents the passive accumulation of integrin receptors into clusters. After initial cell contact with immobilized ligand, a dynamic, diffusion-dependent accumulation of clustered integrins may be needed to augment the overall cellular avidity for the ligand-coated surface. Notably, clustering deficiencies for the X4C0 integrin, directly measured here at 4°C, are consistent with an indirectly measured deficiency in X4C0 clustering seen previously at 37°C (18). In that case, X4C0 was defective in mediating antibody-redirected cell adhesion, a process dependent on mAb bridging between Fc receptors and clustered integrins (18).

How might α tail deletion cause decreased diffusivity leading to reduced clustering? We propose that the α chain cytoplasmic domain covers a negative site in the integrin β chain tail. Consistent with this model, it was previously shown that various integrin α chain tails can shield β chain tails from critical interactions with cytoskeletal proteins (32–34), whereas at the same time, α chains tails often make positive contributions to cell adhesion (9, 10, 35–37). Most likely, the unshielded and unregulated interactions of β tails with cytoskeletal proteins may lead to increased constitutive cytoskeletal anchoring, and thus diminished diffusion and clustering at adhesive sites. Supporting this notion, low doses of cytochalasin D markedly increased adhesion of truncated $\alpha^4\beta_1$, but not wild-type $\alpha^4\beta_1$. The range of cytochalasin D concentrations that promoted X4C0 adhesion (0.01–1 μg/ml) is consistent with previously published cytochalasin D concentrations that stimulated $\alpha^L\beta_2$–mediated adhesion (7).

The overall importance of both diffusion and clustering to cell adhesion has been noted previously. For example, increases in the diffusion and lateral mobility of $\alpha^L\beta_2$ (7) and LFA-3 (38) correlate with increases in cell adhesion and adhesion strengthening, respectively. Furthermore, in-

tegrin clustering is necessary for full integrin signaling (39), and clustering of $\alpha^M\beta_2$ and $\alpha^L\beta_2$ integrins promoted by phorbol ester or calcium also correlates with increased integrin-mediated adhesion (40, 41).

Regulation of integrin diffusion/clustering may be highly relevant towards the understanding of inside–out signaling mechanisms for β_1 and β_2 integrins, especially when affinity modulation is not involved. For example, stimulation of $\alpha^4\beta_1$–mediated adhesion with macrophage inflammatory protein-1β or with anti-CD3 or anti-CD31 antibodies did not detectably induce binding of soluble VCAM (26), and phorbol esters stimulated adhesion mediated by $\alpha^5\beta_1$, $\alpha^M\beta_2$, and $\alpha^L\beta_2$ without affecting soluble ligand binding (42–45). Notably, the effects of phorbol ester stimulation and integrin α^4 tail deletion show a striking parallel. Like α^4 tail deletion, phorbol esters also (*a*) fail to alter integrin affinity for ligand, (*b*) fail to alter $\alpha^4\beta_1$–dependent tethering under shear (11, 12), but (*c*) markedly regulate static cell adhesion and adhesion strengthening under hydrodynamic flow (11), and (*d*) regulate integrin diffusion rates (7). However, whereas α^4 tail deletion leads to increased cytoskeletal restraints and diminished lateral diffusion, phorbol ester appears to release active cytoskeletal restraints, thereby increasing lateral diffusion of the $\alpha^L\beta_2$ integrin (7). Together, these results emphasize that a diffusion/clustering mechanism may be of general importance for regulating adhesion, especially in the absence of changes in ligand binding (26). Also, impaired integrin diffusion/clustering may at least partly explain loss of cell adhesion observed upon the deletion of other integrin α chain cytoplasmic domains (35–37).

In conclusion, this report demonstrates that an integrin mutation can alter cell adhesion by a selective effect on receptor diffusion and clustering. In addition, the results strongly suggest that integrin cytoplasmic domains are critical for control of integrin diffusivity and clustering. We propose that control of cell adhesion at the level of integrin clustering is likely to be an important component of inside–out signaling, especially in cases when ligand binding is not altered.

We thank Dr. Roy Lobb (Biogen, Inc., Cambridge, MA) for providing recombinant soluble VCAM and VCAM–Ig–AP, Dr. Philip Lake (Sandoz Co., East Hanover, NJ) for providing VCAM-κ, and Dr. Ted Yednock (Athena Neurosciences, San Francisco, CA) for providing mAb 15/7.

This work was supported by a research grant (GM46526 to M.E. Hemler) and a postdoctoral fellowship (AI09490 to R.L. Yauch) from the National Institutes of Health. D.P. Felsenfeld was supported by the Cancer Research Fund of the Damon Runyon-Walter Winchell Foundation Fellowship.

Address correspondence to Martin E. Hemler, Rm. M-613, Dana-Farber Cancer Institute, 44 Binney St., Boston, MA 02115.

Received for publication 26 November 1996 and in revised form 11 July 1997.

References

1. Hynes, R.O. 1992. Integrins: versatility, modulation and signalling in cell adhesion. *Cell*. 69:11–25.
2. Schwartz, M.A., M.D. Schaller, and M.H. Ginsberg. 1995. Integrins: emerging paradigms of signal transduction. *Annu. Rev. Cell Dev. Biol.* 11:549–599.
3. Hughes, P.E., F. Diaz-Gonzalez, L. Leong, C. Wu, J.A. McDonald, S.J. Shattil, and M.H. Ginsberg. 1996. Breaking the integrin hinge: a defined structural constraint regulates integrin signaling. *J. Biol. Chem.* 271:6571–6574.
4. Peter, K., and T.E. O'Toole. 1995. Modulation of cell adhesion by changes in αLβ2 (LFA-1, CD11A/CD18) cytoplasmic domain/cytoskeletal interaction. *J. Exp. Med.* 181:315–326.
5. Faull, R.J., and M.H. Ginsberg. 1995. Dynamic regulation of integrins. *Stem Cells.* 13:38–46.
6. Stewart, M., and N. Hogg. 1996. Regulation of leukocyte integrin function: affinity vs. avidity. *J. Cell. Biochem.* 61:554–561.
7. Kucik, D.F., M.L. Dustin, J.M. Miller, and E.J. Brown. 1996. Adhesion-activating phorbol ester increases the mobility of leukocyte integrin LFA-1 in cultured lymphocytes. *J. Clin. Invest.* 97:2139–2144.
8. Lub, M., Y. Van Kooyk, and C.G. Figdor. 1995. Ins and outs of LFA-1. *Immunol. Today.* 16:479–483.
9. Kassner, P.D., and M.E. Hemler. 1993. Interchangeable α chain cytoplasmic domains play a positive role in control of cell adhesion mediated by VLA-4, a β_1-integrin. *J. Exp. Med.* 178:649–660.
10. Kassner, P.D., S. Kawaguchi, and M.E. Hemler. 1994. Minimum α chain sequence needed to support integrin-mediated adhesion. *J. Biol. Chem.* 269:19859–19867.
11. Alon, R., P.D. Kassner, M.W. Carr, E.B. Finger, M.E. Hemler, and T.A. Springer. 1995. The integrin VLA-4 supports tethering and rolling in flow on VCAM-1. *J. Cell Biol.* 128:1243–1253.
12. Kassner, P.D., R. Alon, T.A. Springer, and M.E. Hemler. 1995. Specialized functional roles for the integrin α^4 cytoplasmic domain. *Mol. Biol. Cell.* 6:661–674.
13. O'Toole, T.E., J. Ylänne, and B.M. Culley. 1995. Regulation of integrin affinity states through an NPXY motif in the β subunit cytoplasmic domain. *J. Biol. Chem.* 270:8553–8558.
14. O'Toole, T.E., Y. Katagiri, R.J. Faull, K. Peter, R.N. Tamura, V. Quaranta, J.C. Loftus, S.J. Shattil, and M.H. Ginsberg. 1994. Integrin cytoplasmic domains mediate inside–out signal transduction. *J. Cell Biol.* 124:1047–1059.
15. Lobb, R.R., G. Antognetti, R.B. Pepinsky, L.C. Burkly, D.R. Leone, and A. Whitty. 1995. A direct binding assay for the vascular cell adhesion molecule-1 (VCAM1) interaction

with α4 integrins. *Cell Adhesion & Commun*. 3:385–397.
16. Hemler, M.E., C. Huang, Y. Takada, L. Schwarz, J.L. Strominger, and M.L. Clabby. 1987. Characterization of the cell surface heterodimer VLA-4 and related peptides. *J. Biol. Chem*. 262:11478–11485.
17. Pujades, C., J. Teixidó, G. Bazzoni, and M.E. Hemler. 1996. Integrin cysteines 278 and 717 modulate VLA-4 ligand binding and also contribute to $\alpha_{4/180}$ formation. *Biochem. J.* 313: 899–908.
18. Weitzman, J.B., C. Pujades, and M.E. Hemler. 1997. Integrin α chain cytoplasmic tails regulate "antibody-redirected" cell adhesion, independent of ligand binding. *Eur. J. Immunol*. 27:78–84.
19. Hemler, M.E., and J.L. Strominger. 1982. Monoclonal antibodies reacting with immunogenic mycoplasma proteins present in human hematopoietic cell lines. *J. Immunol*. 129: 2734–2738.
20. Yednock, T.A., C. Cannon, C. Vandevert, E.G. Goldbach, G. Shaw, D.K. Ellis, C. Liaw, L.C. Fritz, and I.L. Tanner. 1995. $\alpha_4\beta_1$ integrin-dependent cell adhesion is regulated by a low affinity receptor pool that is conformationally responsive to ligand. *J. Biol. Chem*. 270:28740–28750.
21. Elices, M.J., L. Osborn, Y. Takada, C. Crouse, S. Luhowskyj, M.E. Hemler, and R.R. Lobb. 1990. VCAM-1 on activated endothelium interacts with the leukocyte integrin VLA-4 at a site distinct from the VLA-4/fibronectin binding site. *Cell*. 60:577–584.
22. Felsenfeld, D.P., D. Choquet, and M.P. Sheetz. 1996. Ligand binding regulates the directed movement of β1 integrins on fibroblasts. *Nature (Lond.)*. 383:438–440.
23. Schmidt, C.E., A.F. Horwitz, D.A. Lauffenburger, and M.P. Sheetz. 1993. Integrin–cytoskeletal interactions in migrating fibroblasts are dynamic, asymmetric, and regulated. *J. Cell Biol*. 123:977–991.
24. Gelles, J., B.J. Schnapp, and M.P. Sheetz. 1988. Tracking kinesin-driven movements with nanometre-scale precision. *Nature (Lond.)*. 331:450–453.
25. Qian, H., M.P. Sheetz, and E.L. Elson. 1997. Single particle tracking. Analysis of diffusion and flow in two-dimensional systems. *Biophys. J.* 60:910–921.
26. Jakubowski, A., M.D. Rosa, S. Bixler, R. Lobb, and L.C. Burkly. 1995. Vascular cell adhesion molecule (VCAM)–Ig fusion protein defines distinct affinity states of the very late antigen-4 (VLA-4) receptor. *Cell Adhesion Commun*. 3:131–142.
27. Masumoto, A., and M.E. Hemler. 1993. Multiple activation states of VLA-4: mechanistic differences between adhesion to CS1/fibronectin and to VCAM-1. *J. Biol. Chem*. 268:228–234.
28. Puzon-Mclaughlin, W., T.A. Yednock, and Y. Takada. 1996. Regulation of conformation and ligand binding function of integrin α5β1 by the β1 cytoplasmic domain. *J. Biol. Chem*. 271:16580–16585.
29. Pulido, R., M.J. Elices, M.R. Campanero, L. Osborn, S. Schiffer, A. García-Pardo, R. Lobb, M.E. Hemler, and F. Sánchez-Madrid. 1991. Functional evidence for three distinct and independently inhibitable adhesion activities mediated by the human integrin VLA-4: correlation with distinct α4 epitopes. *J. Biol. Chem*. 266:10241–10245.
30. Kucik, D.F., E.L. Elson, and M.P. Sheetz. 1989. Forward transport of glycoproteins on leading lamellipodia in locomoting cells. *Nature (Lond.)*. 340:315–317.
31. Bazzoni, G., D.-T. Shih, C.A. Buck, and M.E. Hemler. 1995. mAb 9EG7 defines a novel β_1 integrin epitope induced by soluble ligand and manganese, but inhibited by calcium. *J. Biol. Chem*. 270:25570–25577.
32. LaFlamme, S.E., S.K. Akiyama, and K.M. Yamada. 1992. Regulation of fibronectin receptor distribution. *J. Cell Biol*. 117:437–447.
33. Briesewitz, R., A. Kern, and E.E. Marcantonio. 1993. Ligand-dependent and -independent integrin focal contact localization: the role of the α chain cytoplasmic domain. *Mol. Biol. Cell*. 4:593–604.
34. Ylänne, J., Y. Chen, T.E. O'Toole, J.C. Loftus, Y. Takada, and M.H. Ginsberg. 1993. Distinct functions of integrin α and β subunit cytoplasmic domains in cell spreading and formation of focal adhesions. *J. Cell Biol*. 122:223–233.
35. Kawaguchi, S., and M.E. Hemler. 1993. Role of the α subunit cytoplasmic domain in regulation of adhesive activity mediated by the integrin VLA-2. *J. Biol. Chem*. 268:16279–16285.
36. Shaw, L.M., and A.M. Mercurio. 1993. Regulation of α6β1 integrin laminin receptor function by the cytoplasmic domain of the α6 subunit. *J. Cell Biol*. 123:1017–1025.
37. Filardo, E.J., and D.A. Cheresh. 1994. A β turn in the cytoplasmic tail of the integrin αv subunit influences conformation and ligand binding of αvβ3. *J. Biol. Chem*. 269:4641–4647.
38. Chan, P.-Y., M.B. Lawrence, M.L. Dustin, L.M. Ferguson, D.E. Golan, and T.A. Springer. 1991. Influence of receptor lateral mobility on adhesion strengthening between membranes containing LFA-3 and CD2. *J. Cell Biol*. 115:245–255.
39. Miyamoto, S., S.K. Akiyama, and K.M. Yamada. 1995. Synergistic roles for receptor occupancy and aggregation in integrin transmembrane function. *Science (Wash. DC)*. 267:883–885.
40. Detmers, P.A., S.D. Wright, E. Olsen, B. Kimball, and Z.A. Cohn. 1987. Aggregation of complement receptors on human neutrophils in the absence of ligand. *J. Cell Biol*. 105: 1137–1145.
41. Van Kooyk, Y., P. Weder, K. Heije, and C.G. Figdor. 1994. Extracellular Ca2+ modulates leukocyte function-associated antigen-1 cell surface distribution on T lymphocytes and consequently affects cell adhesion. *J. Cell Biol*. 124:1061–1070.
42. Danilov, Y.N., and R.L. Juliano. 1989. Phorbol ester modulation of integrin-mediated cell adhesion: a postreceptor event. *J. Cell Biol*. 108:1925–1933.
43. Faull, R.J., N.L. Kovach, J.M. Harlan, and M.H. Ginsberg. 1994. Stimulation of integrin-mediated adhesion of T lymphocytes and monocytes: two mechanisms with divergent biological consequences. *J. Exp. Med*. 179:1307–1316.
44. Altieri, D.C., and T.S. Edgington. 1988. The saturable high affinity association of factor X to ADP-stimulated monocytes defines a novel function of the Mac-1 receptor. *J. Biol. Chem*. 263:7007–7015.
45. Stewart, M.P., C. Cabañas, and N. Hogg. 1996. T cell adhesion to intercellular adhesion molecule-1 (ICAM-1) is controlled by cell spreading and the activation of integrin LFA-1. *J. Immunol*. 156:1810–1817.